

COMMUNICATION

[View Article Online](#)
[View Journal](#) | [View Issue](#)

Cite this: *Polym. Chem.*, 2020, **11**, 7009

Received 30th August 2020,
Accepted 23rd October 2020

DOI: 10.1039/d0py01233e

rsc.li/polymers

Mechanism and application of surface-initiated ATRP in the presence of a Zn⁰ plate†

Rebecca Faggion Albers,^a Wenqing Yan,^b Matteo Romio,^{b,c} Edson R. Leite,^{d,e} Nicholas D. Spencer,^b Krzysztof Matyjaszewski^f and Edmondo M. Benetti^{*b,c}

Surface-initiated atom transfer radical polymerization in the presence of a Zn⁰ plate (SI-Zn⁰-ATRP) enables the rapid synthesis of chemically diverse polymer brushes from both planar inorganic supports, and fabrics made of natural fibers. This process enables the controlled formation of polymer-brush layers on a variety of substrates, without the need for either inert conditions or lengthy deoxygenation procedures of the reaction mixtures.

The development of oxygen-tolerant, surface-initiated, controlled radical polymerization (SI-CRP) methods has paved the way for the accessible synthesis of polymer-brush coatings on large substrates, circumventing the need for lengthy deoxygenation of reaction mixtures. Following closely the recent advances in the development of oxygen-tolerant CRPs in solution,¹ the application of analogous processes to solid surfaces has offered the possibility to translate the synthesis of polymer brushes from fundamental studies into technologically relevant processes.

Similarly to solution-based approaches, the successful and controlled fabrication of polymer brushes under ambient conditions has been accomplished by employing oxygen scavengers. For instance, in the presence of appropriate reducing agents, Cu-based catalysts efficiently consume oxygen through complexation and can still trigger the growth of composition-

ally different brushes during surface-initiated activators regenerated by electron transfer atom transfer radical polymerization (SI-ARGET ATRP).^{2–7} Alternatively, in the presence of visible or UV light, oxygen can be consumed by organic or organometallic photocatalysts that are typically employed during photoinduced SI-ATRP,^{8,9} or photoinduced electron-transfer surface-initiated reversible addition fragmentation chain transfer polymerization (SI-PET RAFT),¹⁰ enabling the rapid fabrication of polymer brushes without degassing the reaction mixtures, while keeping polymerization setups exposed to air.

Besides scavengers present in solution, oxygen can be alternatively consumed by applying zerovalent metal (Mt⁰)-coated plates, which consume oxygen to form oxide layers, and simultaneously act as source of transition-metal catalyst for ATRP when placed on initiator-bearing surfaces previously covered by a thin layer of monomer/ligand mixtures.^{11–18}

Following this strategy, Jordan and co-workers introduced Cu⁰-mediated SI-ATRP, demonstrating how this process can be applied for the modification of extremely large substrates, by simply keeping them on a lab bench, and using just microliter volumes of polymerization mixtures.^{11,19} This process enabled the extremely rapid synthesis of compositionally different polymer brushes²⁰ from a variety of inorganic and organic supports.^{16,21}

Relevantly, when Cu⁰-coated plates were replaced with Fe⁰-coated surfaces thick brush films could be grown in a biocompatible process—even from supports pre-seeded with mammalian cells, without altering their viability.¹⁸

Motivated by the possibility to expand this method to alternative, readily accessible and inexpensive Mt⁰ plates, in this work we explore the applicability of Zn⁰ plates to favor the fast and oxygen-tolerant fabrication of thick brush films.

As previously demonstrated in the case of polymerizations performed in solution, Zn⁰ powder efficiently acts as reducing agent for Cu^{II} during supplemental activator and reducing agent (SARA) ATRP,^{22–24} showing a very high reducing activity when compared to Fe⁰ or Mg⁰.²⁵

^aComplex Materials, Department of Materials, ETH Zürich, Vladimir-Prelog-Weg 1-5/10, CH-8093 Zurich, Switzerland

^bLaboratory for Surface Science and Technology, Department of Materials, ETH Zürich, Vladimir-Prelog-Weg 1-5/10, CH-8093 Zurich, Switzerland.
E-mail: edmondo.benetti@mat.ethz.ch

^cSwiss Federal Laboratories for Materials Science and Technology (Empa), Lerchenfeldstrasse 5, CH-9014 St. Gallen, Switzerland

^dDepartment of Chemistry, Federal University of São Carlos, 13565-905 São Carlos, SP, Brazil

^eBrazilian Nanotechnology National Laboratory (LNNano), Brazilian Center for Research in Energy and Materials (CNPem), 13083-970 Campinas, Brazil

^fDepartment of Chemistry, Carnegie Mellon University, 4400 Fifth Avenue, Pittsburgh, USA

†Electronic supplementary information (ESI) available. See DOI: 10.1039/d0py01233e





Scheme 1 (a) Mechanism of SI-Zn⁰-ATRP. A polymerization mixture comprising monomer, solvent, ligand, and Cu^{II}Br₂ is placed in between an ATRP-initiator-functionalized SiO_x substrate and a Zn⁰ plate. The metallic surface consumes oxygen through the formation of Zn^{II}O [1]. Simultaneously, it acts as reducing agent for Cu^{II}Br₂/L, generating Cu^IBr/L activators, which diffuse through the reaction mixture and trigger the controlled growth of polymer grafts [2]. Zn⁰ particles leaching from the metal plate can act as supplemental activators in the presence of ligand [3], initiating polymerization from the surface and simultaneously providing Zn^{II}Br₂/L species. (b) Polymer brush films can be grafted from SiO_x substrates previously functionalized with ATRP initiator.

In the case of the synthesis of polymer brushes from planar substrates, polymerization mixtures including monomer, ligand, Cu^{II}Br₂ and solvent are sandwiched between an ATRP initiator-modified SiO_x substrate, and a Zn⁰ plate.

The metallic plate was polished just before the experiment (Scheme 1) in order to remove the native oxide layer, and to generate an homogeneous metal surface (ESI[†]). After this process, a reaction volume of ~1 μL cm⁻² is generated between the two opposing surfaces, and the vertical spacing between the initiator-bearing substrate and the Zn⁰ plate (d) corresponds to ~10 μm.¹⁷

Under these conditions, oxygen dissolved in the polymerization solution is rapidly consumed through oxidation of Zn⁰ to Zn^{II}O (Scheme 1a [1]),^{26,27} while Cu^{II}Br₂/L species are simultaneously reduced to Cu^IBr/L adducts. These can diffuse in the medium and reach the initiator-functionalized surface, triggering the controlled growth of polymer chains according to the ATRP equilibrium (Scheme 1a [2]).

Surface-initiated Zn⁰-mediated ATRP (SI-Zn⁰-ATRP) of (oligoethylene glycol)methacrylate (OEGMA) was exemplarily investigated. A 50% (v/v) solution of OEGMA in dimethylformamide (DMF) containing 10 mM Cu^{II}Br₂ and 10 mM tris (2-pyridylmethyl)amine (TPMA) was poured on a freshly polished Zn⁰ plate, and subsequently covered by a SiO_x substrate, which had previously been functionalized with a silane-based ATRP initiator. Variable-angle spectroscopic ellipsometry (VASE) was employed to monitor the increment in POEGMA-brush dry thickness (*T_{dry}*) *ex situ*, providing an insight into brush-growth kinetics. As reported in Fig. 1a, SI-Zn⁰-ATRP enabled the rapid and progressive growth of POEGMA brushes, which reached more than 270 nm of dry thickness after 90 min of reaction. No induction time was recorded, suggesting a very fast reduction of Cu^{II}Br₂/L species by Zn⁰,²⁶ and a rapid diffusion of activators to the initiator sites at the substrate.



Fig. 1 Dry thickness of polymer brushes synthesized by SI-Zn⁰-ATRP and measured by VASE. (a) Dry thickness of POEGMA brushes after different polymerization times, using a 50% OEGMA (v/v) solution in DMF, 10 mM TPMA, with and without 10 mM Cu^{II}Br₂. (b) Dry thickness of PMMA brushes synthesized by using a mixture of 50% MMA (v/v) in DMF, and 10 mM Cu^{II}Br₂/TPMA. Values of dry thickness are expressed as mean ± SD (*n* = 4).

It is important to emphasize that the preparation of Zn⁰ plates by polishing is a standard procedure for treating metal surfaces and requires just 15–20 minutes, and (rather cheap) sandpaper. After this process, 20 × 20 cm² activated Zn⁰ plates (typical cost ~2 €) are obtained. These can be used multiple times and for grafting brushes on a relatively large number of substrates.

Similarly to POEGMA analogues, the growth of poly(methyl methacrylate) (PMMA) brushes by SI-Zn⁰-ATRP (50% v/v in DMF, with 10 mM Cu^{II}Br₂/TPMA) followed an initially fast kinetics, without an induction period (Fig. 1b). However, the rate of PMMA-brush thickening significantly slowed down after ~60 min, and PMMA films reached a dry thickness of ~40 nm after two hours of reaction.

Interestingly, when SI-Zn⁰-ATRP was performed in the absence of Cu^{II}Br₂ but in the presence of ligand, significant



brush growth could still be recorded. As shown in Fig. 1a, POEGMA brushes reached nearly 150 nm of dry thickness when a mixture including 50% OEGMA and 10 mM TPMA was sandwiched between a Zn^0 plate and an ATRP initiator-bearing substrate for 90 min.

This result suggests that Zn^0 can act as supplemental activator during the growth of polymer brushes by SI- Zn^0 -ATRP, in agreement with the mechanism of SARA ATRP studied in solution in the presence of Zn^0 particles.²⁵

Considering the physical distance between the Zn^0 plate and the ATRP initiator-functionalized substrate within an ideal polymerization setup, we hypothesize that Zn^0 micro/nanoparticles produced during the polishing process (Fig. S1†) might diffuse within the polymerization medium and in the presence of ligand can activate surface-bound initiators, triggering brush growth (Scheme 1a [3]). In particular, Zn^0/L adducts can act as supplemental activators reacting with alkyl halides and generating radicals that can initiate polymerization from the surface. However, this process simultaneously produces $\text{Zn}^{\text{II}}\text{Br}_2/\text{L}$ species, which are very poor deactivators, presumably leading to a redox-initiated free radical surface-initiated polymerization process.²⁵

Hence, Cu^{II} -based species added in solution are fundamental to guarantee a controlled and steady growth of polymer brushes. The role of $\text{Cu}^{\text{II}}\text{Br}_2/\text{L}$ during SI- Zn^0 -ATRP can be elucidated by measuring the dry thickness of POEGMA and PMMA brushes obtained after a fixed polymerization time of 30 min, while varying $[\text{Cu}^{\text{II}}\text{Br}_2/\text{L}]$ initially added in the mixture. As reported in Fig. 2a, both POEGMA- and PMMA-brush thicknesses significantly increase with $[\text{Cu}^{\text{II}}\text{Br}_2/\text{L}]$ until a maximum in T_{dry} is reached, in correspondence to a value of $[\text{Cu}^{\text{II}}\text{Br}_2/\text{L}] \sim 10$ mM. When $[\text{Cu}^{\text{II}}\text{Br}_2/\text{L}]$ is further increased, the values of T_{dry} progressively decrease, indicating that an “optimum” con-

centration of Cu^{II} -based species enables the fastest growth of polymer brushes through SI- Zn^0 -ATRP.

On the one hand, an initial increment in $[\text{Cu}^{\text{II}}\text{Br}_2/\text{L}]$ results in a concomitant increase in $[\text{Cu}^{\text{I}}\text{Br}/\text{L}]$ through the rapid reduction by Zn^0 , determining a faster polymerization and thus the formation of thicker brushes. On the other hand, a further increase in $[\text{Cu}^{\text{II}}\text{Br}_2/\text{L}]$ beyond 10 mM presumably causes accumulation of deactivators, which necessarily slows down the grafting process and lead to the formation of thinner films.

Hence, the balance between generation of activator species by Zn^0 -mediated reduction and accumulation of Cu^{II} -based deactivators, determines the brush-growth kinetics during SI- Zn^0 -ATRP.

Under optimized conditions, SI- Zn^0 -ATRP enabled the synthesis of chemically different polymer brushes by simply performing the grafting process on a Petri dish exposed to air and placed on a lab bench, using just few microliter volumes of reaction solutions, and without the need for their deoxygenation. In this way, poly(methacrylate), poly(acrylate), poly(acrylamide) and poly(styrene) brushes could be fabricated and under full ambient conditions (Fig. 2b). In particular poly(*N*-isopropylacrylamide) (PNIPAM), poly(2-methacryloyloxyethyltrimethylammonium chloride) (PMETAC) and poly(2-methacryloyloxyethyl phosphorylcholine) (PMPC) brushes with thicknesses ≥ 30 nm were synthesized following relatively short reaction times. In contrast, poly(styrene) (PS) and poly(butyl acrylate) (PBA) brushes showed just ~ 10 nm of dry thickness, presumably due to the relatively low temperature applied during the grafting process.

It is also important to emphasize that with respect to the corresponding grafting process employing Cu^0 plates, SI- Zn^0 -ATRP enables the controlled grafting of polymer brushes while applying reaction environments that could virtually display relatively low toxicity. In order to confirm this hypothesis, besides $\text{Cu}^{\text{II}}/\text{Cu}^{\text{I}}$ species, the rapid growth of POEGMA brushes could be accomplished by applying a Fe-based catalyst. In particular, $\text{Fe}^{\text{III}}\text{Br}_3/\text{tertbutylammonium bromide}$ (TBABr) is readily reduced to $\text{Fe}^{\text{II}}\text{Br}_2/\text{TBABr}$ activators by the Zn^0 surface, triggering the growth of more than 30 nm-thick POEGMA brushes in just 60 min of reaction (Fig. S2†). Relevantly, a similar result was previously accomplished by using Fe^0 plates as reducing agent for Fe^0 -mediated SI-ATRP (SI- Fe^0 -ATRP).¹⁹ However, in contrast to SI- Fe^0 -ATRP, in SI- Zn^0 -ATRP the grafting process is mediated by metallic plates based on Zn^0 , which are much cheaper (2 vs. 60 € for a $20 \times 20 \text{ cm}^2$ plate) and more readily available with respect to Fe^0 or Fe^0 -coated analogues.

In order to demonstrate the applicability of SI- Zn^0 -ATRP for the modification of a variety of supports, we subsequently investigated the growth of polymer brushes from cotton-based wound dressings, which had previously been modified with ATRP initiator moieties. 100%-cotton fabrics functionalized with α -bromoisobutyrate functions were initially soaked in a polymerization mixture comprising 50% (v/v) OEGMA in DMF and 10 mM $\text{Cu}^{\text{II}}\text{Br}_2/\text{TPMA}$, and subsequently sandwiched between a Zn^0 plate and an inert glass slide. Attenuated total

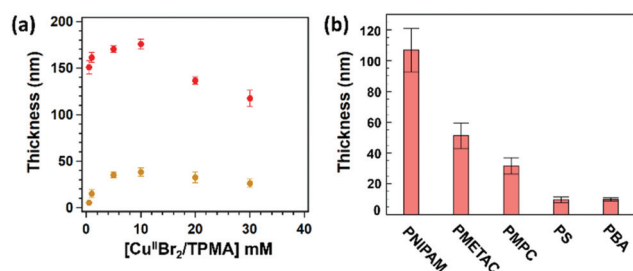


Fig. 2 (a) Dry thickness of POEGMA (red markers) and PMMA brushes (yellow markers) synthesized by SI- Zn^0 -ATRP keeping a constant polymerization time of 30 min, and by varying $[\text{Cu}^{\text{II}}\text{Br}_2/\text{TPMA}]$. Values of dry thickness are expressed as mean \pm SD ($n = 4$). (b) Dry thickness of chemically different polymer brushes synthesized by SI- Zn^0 -ATRP. Poly(*N*-isopropylacrylamide) (PNIPAM) (conditions: 3 M NIPAM, 10 mM TPMA, 10 mM $\text{Cu}^{\text{II}}\text{Br}_2$ in DMSO for 30 min); poly(2-methacryloyloxyethyltrimethylammonium chloride) (PMETAC) (1.5 M METAC, 10 mM TPMA, 10 mM $\text{Cu}^{\text{II}}\text{Br}_2$, 10 mM NaBr in H_2O for 120 min); poly(2-methacryloyloxyethyl phosphorylcholine) (PMPC) (1.5 M MPC, 20 mM 2,2'-bipyridyl, 10 mM $\text{Cu}^{\text{II}}\text{Br}_2$ in methanol, for 180 min); poly(styrene) (PS) (20% v/v styrene, 10 mM TPMA, 10 mM $\text{Cu}^{\text{II}}\text{Br}_2$, in DMF, for 180 min); poly(butyl acrylate) (PBA) (20% v/v BA, 10 mM tris[2-(dimethylamino)ethyl]amine, 10 mM $\text{Cu}^{\text{II}}\text{Br}_2$ in DMF, for 180 min).





Fig. 3 (a) ATR-FTIR spectra from unmodified cotton fabrics (cotton), ATRP-initiator-functionalized cotton (cotton-Br), POEGMA brush-functionalized cotton after 2 h (cotton-POEGMA 2 h) and 8 h (cotton-POEGMA 8 h) of SI-Zn⁰-ATRP. (b) Values of transmittance of C=O band as a function of polymerization time. Scanning electron micrographs recorded on unmodified cotton (c, d), cotton-Br (e, f), cotton-POEGMA 2 h (g, h), and cotton-POEGMA 8 h (i, j).

reflection Fourier-transform infrared spectroscopy (ATR-FTIR) confirmed the successful grafting of POEGMA brushes from the cotton fibers after 2 and 8 hours of reaction (Fig. 3a), through the appearance of the C=O stretching band at 1717 cm⁻¹, the C-H band at 2869 cm⁻¹ and the C-O signals at 1248 and 1102 cm⁻¹. In addition, the decrease in the values of transmittance of the C=O band with polymerization time suggested the progressive growth of POEGMA grafts. The formation of brush layers on the cotton fibers was additionally confirmed by scanning electron microscopy (SEM). As reported in Fig. 2c-f, the surface morphology of cotton fibers did not show a significant variation after functionalization with ATRP initiator. However, following SI-Zn⁰-ATRP, a uniform brush film became visible on the cotton structures, and grew thicker after relatively long polymerization times.

activators that in the presence of ligand diffuse to the initiator-bearing substrate, and lead to the rapid growth of polymer grafts, which proceeds according to the ATRP equilibrium. Zn⁰ micro/nanoparticles leaching from the metallic surface can additionally act as supplemental activators while diffusing through the polymerization mixture. In the absence of Cu^{II} species, Zn⁰/L centers trigger a redox-initiated, free-radical polymerization process, through the simultaneous generation of poor deactivators based on ZnBr₂/L adducts.

Under optimized experimental conditions, SI-Zn⁰-ATRP enables the rapid polymerization of different monomer species (acrylates, methacrylates, acrylamides and styrene), it is compatible with both Cu- and Fe-based catalysts, and it could be applied from model inorganic substrates as well as for the modification of three-dimensional fabrics, such as in the case of cotton-based wound dressings.

Conclusions

SI-Zn⁰-ATRP represents an extremely versatile method to synthesize chemically different polymer brushes under full ambient conditions, using just microliter volumes of reaction solutions, and without the need for their previous deoxygenation. When a polymerization mixture including Cu^{II} salts, ligand and monomer is sandwiched between a Zn⁰ plate and a SiO_x substrate functionalized with ATRP initiators oxygen is rapidly consumed *via* the formation of Zn^{II}O. Simultaneously, Cu^{II}-based species are reduced by the Zn⁰ plate, yielding Cu^I

Experimental section

Materials

Silicon wafers (P/B<100>) were purchased from Si-Mat Silicon Wafers (Germany), Zn plates were purchased from Mayitr. 3-(Aminopropyl)triethoxysilane (APTES, ≥98%, Sigma-Aldrich), 2-bromoisobutyl bromide (BiBB, 98%, Sigma-Aldrich), triethylamine (TEA, ≥99.5%, Sigma-Aldrich), dichloromethane (DCM, dry, ≥99.8%, Acros), cotton fabrics (100%, Rhena® Ideal), tris(2-pyridylmethyl)amine (TPMA, 98%, Sigma



Aldrich), 2,2'-bipyridyl (bipy, ≥, Sigma-Aldrich), tris(2-dimethylaminoethyl)amine (Me₆TREN, 99%, ABCR), Cu^{II}Br₂ (99%, Sigma Aldrich), 2-methacryloyloxyethyl phosphorylcholine (MPC, 97%, Sigma-Aldrich), [2-(methacryloyloxy)ethyl]trimethylammonium chloride solution (METAC, 80% in water, Sigma-Aldrich), and tetrahydrofuran (dry THF, 99.5%, Acros), were used as received. Water used in all experiments was from Millipore Milli-Q. Oligo(ethylene glycol)methacrylate (OEGMA, $M_n \sim 500$, Sigma-Aldrich), methyl methacrylate (MMA, 99%, Sigma-Aldrich), styrene (99.5%, Acros Organics) and butyl acrylate (BA, 99%, Acros Organics) were purified by passing them through a basic alumina column. *N*-Isopropylacrylamide (NIPAM, >98.0%, Tokyo Chemical Industry) was recrystallized from toluene to remove inhibitors.

Methods

Functionalization of SiO_x substrates. Silicon substrates (Si-Mat Silicon Wafers, Germany) were cleaned with piranha solution (3:1 H₂SO₄:H₂O₂) for 30 min, and subsequently washed extensively with ultra-pure water. The substrates were first functionalized with APTES, through vapor deposition, and they were subsequently washed with dry toluene and ultra-pure water. Later on, SiO_x-APTES substrates were placed in a flask kept under N₂ atmosphere, in which dry DCM, BIBB (1 v%) and TEA (1 v%) were added. The reaction was carried out for one hour, and the substrates were finally washed with chloroform and ethanol, yielding ATRP initiator-functionalized SiO_x surfaces.

Zn⁰ plate preparation. Zn⁰ plates were first grinded with Struers SiC foils, presenting grit sizes of 320, 500, 800, 1200, 2000 and 4000 (FEPA). Later on, they were polished with a cloth-coated disc (MD-Mol) using a diamond suspension with a grain size of 3 μm, and finally washed twice with 2-propanol in an ultrasonic bath for 15 min.

SI-Zn⁰-ATRP. A polymerization mixture was placed dropwise on a polished Zn⁰ plate, and ATRP initiator-functionalized substrates were placed on top of that, with a dead weight producing a pressure of 6 g cm⁻² to hold the substrate against the Zn⁰ plate. After the polymerization, the substrates were washed with ethanol (POEGMA), water and methanol (PMPC and PMETAC), toluene and dichloromethane (PS and PBA), finally dried with a N₂ flux and analyzed by VASE.

Grafting from cotton. Cotton fabrics were dried under vacuum overnight in a two-neck round-bottom flask and later on functionalized with ATRP initiator. Namely, 2.0 g of cotton, 100 mL of dry THF, 5 mL of TEA and 0.6 g of DMAP were added to the flask, the system was cooled down to 0 °C and 2.2 mL of BIBB were added dropwise. The suspension was stirred at 0 °C for 2 h, and at room temperature for 24 h.²⁸ The cotton was washed extensively with THF, water and ethanol and dried under vacuum. The resulting ATRP initiator-functionalized cotton was soaked in the polymerization mixture and sandwiched between a Zn⁰ plate and an inert glass slide.

Following polymerization, brush-modified cotton fabrics were subjected to soxhlet extraction with ethanol as solvent to remove any unreacted monomer/unbound polymer.

Variable-angle spectroscopic ellipsometer (VASE). The dry thickness of polymer brush films was determined using a M-2000F John Woollam variable angle spectroscopic ellipsometer (VASE, SENTECH Instruments GmbH), equipped with a He-Ne laser source ($\lambda = 633$ nm, J.A. Woollam Co., Lincoln, NE). The values of amplitude (Ψ) and phase (Δ) were acquired by focusing lenses at 70° from the surface normal as a function of wavelength (350–800 nm). Raw data were fitted with a three-layer model, using bulk dielectric functions for Si and SiO₂ (software WVASE32, LOT Oriel GmbH, Darmstadt, Germany). The polymer-brush layers were analyzed based on a Cauchy model: $n = A + B\lambda^{-2}$, where n is the refractive index, λ is the wavelength, and A and B are assumed to be 1.45 and 0.01, respectively, as values for transparent organic films.

The values of dry thickness of polymer brushes were obtained from 4 different substrates analyzed after SI-Zn⁰-ATRP. At least 3 different points on each substrate were measured by VASE.

Attenuated total reflection fourier-transform infrared spectroscopy (ATR-FTIR). The ATR-FTIR spectra were recorded using an Alpha, Bruker spectrometer, equipped with a diamond crystal. The material was pressed onto the crystal and 64 scans were acquired with a resolution 4 cm⁻¹.

Scanning electron microscopy (SEM). Cotton fabrics were sputter-coated with 5 nm of Pt to avoid charging effects during analysis (CCU-010, Safematic). The micrographs were acquired using a scanning electron microscope (SEM, LEO 1530, Zeiss GmbH, Germany).

Conflicts of interest

There are no conflicts to declare.

Acknowledgements

We thank Prof André R. Studart, Dr Rafael Libanori (ETH Zürich) and Prof. Katharina Maniura (EMPA) for the fruitful scientific discussions. We acknowledge the funding Brazilian agency Fundação de Amparo à Pesquisa do Estado de São Paulo – FAPESP (2016/14493-7 and 2017/22304-2) and EMPA for the financial support.

References

- 1 J. Yeow, R. Chapman, A. J. Gormley and C. Boyer, *Chem. Soc. Rev.*, 2018, **47**, 4357–4387.
- 2 K. Matyjaszewski, H. C. Dong, W. Jakubowski, J. Pietrasik and A. Kusumo, *Langmuir*, 2007, **23**, 4528–4531.
- 3 G. J. Dunderdale, C. Urata, D. F. Miranda and A. Hozumi, *ACS Appl. Mater. Interfaces*, 2014, **6**, 11864–11868.
- 4 T. Sato, G. J. Dunderdale, C. Urata and A. Hozumi, *Macromolecules*, 2018, **51**, 10065–10073.
- 5 N. Li, T. Li, X. Y. Qiao, R. Li, Y. Yao and Y. K. Gong, *ACS Appl. Mater. Interfaces*, 2020, **12**, 12337–12344.



- 6 D. Hong, H. C. Hung, K. Wu, X. J. Lin, F. Sun, P. Zhang, S. J. Liu, K. E. Cook and S. Y. Jiang, *ACS Appl. Mater. Interfaces*, 2017, **9**, 9255–9259.
- 7 H. Kang, W. Jeong and D. Hong, *Langmuir*, 2019, **35**, 7744–7750.
- 8 B. Narupai, Z. A. Page, N. J. Treat, A. J. McGrath, C. W. Pester, E. H. Discekici, N. D. Dolinski, G. F. Meyers, J. R. de Alaniz and C. J. Hawker, *Angew. Chem., Int. Ed.*, 2018, **57**, 13433–13438.
- 9 W. Q. Yan, S. Dadashi-Silab, K. Matyjaszewski, N. D. Spencer and E. M. Benetti, *Macromolecules*, 2020, **53**, 2801–2810.
- 10 M. Li, M. Fromel, D. Ranaweera, S. Rocha, C. Boyer and C. W. Pester, *ACS Macro Lett.*, 2019, **8**, 374–380.
- 11 T. Zhang, Y. Du, F. Muller, I. Amin and R. Jordan, *Polym. Chem.*, 2015, **6**, 2726–2733.
- 12 E. S. Dehghani, Y. H. Du, T. Zhang, S. N. Ramakrishna, N. D. Spencer, R. Jordan and E. M. Benetti, *Macromolecules*, 2017, **50**, 2436–2446.
- 13 Y. J. Che, T. Zhang, Y. H. Du, I. Amin, C. Marschelke and R. Jordan, *Angew. Chem., Int. Ed.*, 2018, **57**, 16380–16384.
- 14 T. Zhang, E. M. Benetti and R. Jordan, *ACS Macro Lett.*, 2019, **8**, 145–153.
- 15 M. Fantin, S. N. Ramakrishna, J. J. Yan, W. Q. Yan, M. Divandari, N. D. Spencer, K. Matyjaszewski and E. M. Benetti, *Macromolecules*, 2018, **51**, 6825–6835.
- 16 W. Q. Yan, M. Fantin, S. Ramakrishna, N. D. Spencer, K. Matyjaszewski and E. M. Benetti, *ACS Appl. Mater. Interfaces*, 2019, **11**, 27470–27477.
- 17 W. Q. Yan, M. Fantin, N. D. Spencer, K. Matyjaszewski and E. M. Benetti, *ACS Macro Lett.*, 2019, **8**, 865–870.
- 18 A. Layadi, B. Kessel, W. Yan, M. Romio, N. D. Spencer, M. Zenobi-Wong, K. Matyjaszewski and E. M. Benetti, *J. Am. Chem. Soc.*, 2020, **142**, 3158–3164.
- 19 T. Zhang, Y. H. Du, J. Kalbacova, R. Schubel, R. D. Rodriguez, T. Chen, D. R. T. Zahn and R. Jordan, *Polym. Chem.*, 2015, **6**, 8176–8183.
- 20 W. Q. Yan, M. Fantin, N. D. Spencer, K. Matyjaszewski and E. M. Benetti, *ACS Macro Lett.*, 2019, **8**, 865–870.
- 21 K. H. Zhang, W. Q. Yan, R. Simic, E. M. Benetti and N. D. Spencer, *ACS Appl. Mater. Interfaces*, 2020, **12**, 6761–6767.
- 22 K. F. Augustine, T. G. Ribelli, M. Fantin, P. Krys, Y. Cong and K. Matyjaszewski, *J. Polym. Sci., Part A: Polym. Chem.*, 2017, **55**, 3048–3057.
- 23 D. Konkolewicz, Y. Wang, M. Zhong, P. Krys, A. A. Isse, A. Gennaro and K. Matyjaszewski, *Macromolecules*, 2013, **46**, 8749–8772.
- 24 D. Konkolewicz, Y. Wang, P. Krys, M. J. Zhong, A. A. Isse, A. Gennaro and K. Matyjaszewski, *Polym. Chem.*, 2014, **5**, 4396–4417.
- 25 Y. Zhang, Y. Wang and K. Matyjaszewski, *Macromolecules*, 2011, **44**, 683–685.
- 26 A. Anastasaki, V. Nikolaou, G. Nurumbetov, P. Wilson, K. Kempe, J. F. Quinn, T. P. Davis, M. R. Whittaker and D. M. Haddleton, *Chem. Rev.*, 2016, **116**, 835–877.
- 27 E. Liarou, R. Whitfield, A. Anastasaki, N. G. Engelis, G. R. Jones, K. Velonia and D. M. Haddleton, *Angew. Chem., Int. Ed.*, 2018, **57**, 8998–9002.
- 28 X. Dong, H. Bao, K. Ou, J. Yao, W. Zhang and J. He, *Fibers Polym.*, 2015, **16**, 1478–1486.

